EXAMPLE 2.3 continued

Table E2.3 Reservoir and Well Data for the Vik No. 1

Initial reservoir pressure	7055 psia
Initial oil FVF	1.5 bbl/STB
Total pay thickness	80 ft
Average permeability	24 md
Initial oil viscosity	0.31 cp
Bubble-point pressure	4800 psia
Wellbore radius (7-in. casing)	0.29 ft
Skin factor before acid treatment	+18.5
Skin factor after-acid treatment	−4.2

This section has discussed only the effect of steady-state or constant skin on the pressure drawdown and production rate. A rate-dependent skin is discussed in the following section. The physical aspects of the skin phenomenon are addressed in chapter 3.

2.4 RATE–PRESSURE RELATION FOR GAS WELLS.

Rawlins and Schellhardt (1936), engineers from the U.S. Bureau of Mines, developed the classic backpressure equation relating gas rate to flowing pressure:

$$q_g = C(p_R^2 - p_{wf}^2)^n. \tag{1.33}$$

The equation was developed after interpreting several hundred multirate gas well tests. A linear trend was observed on a log–log plot of rate versus delta pressure-squared, $p_R^2 - p_{wf}^2$. At the time equation (1.33) was initially suggested, it was not obvious why pressure-squared, instead of pressure, should be used. Nor was it obvious why the exponent n was limited to a value between 0.5 and 1.0. Also absent from the early pioneers' work was an expression for C in terms of reservoir rock and fluid properties (when $n < 1.0$). Yet, even without theoretical argumentation, the backpressure equation received immediate, widespread acceptance and use by the gas industry.

Today we have a better understanding of the backpressure equation. We know that pressure squared accounts for the pressure dependence of fluid properties ($1/\mu_g B_g$ or $p/\mu_g Z$). The backpressure exponent n accounts for high-velocity flow e.g., turbulence. (Note that n equals the reciprocal of the slope of the backpressure straight line.) Although the constant C has yet to be expressed analytically in terms of reservoir properties for cases other than $n = 1$, we know that it accounts for reservoir rock and fluid properties, flow geometry, and transient effects.

Several testing methods can be used to determine the backpressure relation for a gas well. They involve flowing the well at several rates, measuring flowing and buildup pressures, and plotting the results as q_g versus $p_R^2 - p_{wf}^2$ on log–log paper. The common multirate sequences include the flow-after-flow, isochronal, and modified isochronal tests. Example 1.7 (see chapter 1) illustrates the procedure for determining n and C from a flow-after-flow multirate test. The procedures for multirate testing are discussed in section 2.7. Here we shall only note that the flow-after-flow test assumes that a stabilized, pseudosteady state is reached before

changing from one rate to the next. In fact, C is not a constant unless stabilized (pseudosteady-state) production exists. Isochronal tests can be at transient conditions during flow periods, but it is mandatory that shut-in periods, which separate flow periods, are of sufficient duration to reach static reservoir pressure at the wellbore. Also, isochronal tests usually are followed immediately by an extended flow period to determine the stabilized backpressure curve. Generally, multirate tests (particularly the modified isochronal test) should be run with increasing rates. Time required to reach stabilized flow varies from well to well. In general, the higher the permeability, the less time it takes to reach stabilization. On the log–log backpressure curve, a changing C is reflected by a gradual shift of the straight line to the left. The classic paper on multirate testing by Cullender (1955) reports multirate data that confirm this transient behavior of C. Cullender also shows how important it is to account for the shifting backpressure curve during a test of a slow-to-stabilize well.

The backpressure equation originated from field observations. This section will show that, for the particular case of a low-pressure gas well with a backpressure coefficient $n = 1$, the equation matches the behavior predicted by Darcy's law. Lower values of n reflect deviations from Darcy's law that affect and often dominate calculations and interpretations of gas well production.

In section 2.1 we noted that Darcy's law breaks down at high flow velocity. Many models were suggested to replace or modify Darcy's law for high-velocity flow. Several models and their experimental background are discussed by Muskat (1937). The most accepted model was proposed by Forchheimer in 1901:

$$dp/dr = av + bv^2, \tag{2.36}$$

where a and b are constants and $v = q/A$ is fluid velocity. Later work by Green and Duwez (1951) and Cornell and Katz (1953) expressed equation (2.36) in terms of fluid and rock properties

$$dp/dr = (\mu/k)v + \beta\rho v^2, \tag{2.37}$$

where

μ = gas viscosity,
ρ = gas density,
k = formation permeability,
β = high velocity coefficient.

The high-velocity coefficient in equation (2.37) is a property of the formation rock that accounts for the deviation from Darcy's law. Equation (2.37) implies that two rock parameters, permeability and the high-velocity coefficient, are needed to express high-velocity flow in reservoirs.

The deviation from Darcy's flow is more pronounced in gas wells than in oil wells. Therefore, it is introduced here for the first time. Section 3.4 is dedicated to high-velocity flow and expands the discussion beyond the short introduction in this section.

In relation to the radial flow equation we should note two major differences

between gas and undersaturated oil flow: (1) gas properties have a strong pressure dependence at low and intermediate pressures, and (2) high-velocity effects are exhibited by gas flow at relatively low rates. It is possible to account for these phenomena in a gas radial flow model to establish inflow performance equations valid for the entire range of reservoir pressure and flow velocity. The gas equations are developed in terms of reservoir parameters and can be used for both production predictions and data interpretation.

We start from Darcy's law in differential form (eq. [2.4]),

$$v_g = \left(\frac{k}{\mu_g}\right)\frac{dp}{dr}.$$

Velocity can be expressed in terms of volumetric rate at standard conditions q_g and gas FVF, B_g $(= TZP_{sc}/pT_{sc})$:

$$v_g = \frac{q_g B_g}{2\pi hr} = \left(\frac{q_g}{2\pi hr}\right)\left(\frac{TZp_{sc}}{pT_{sc}}\right). \tag{2.38}$$

Substituting equation (2.38) in equation (2.4), separating variables (pressure p and radius r), defining inner and outer boundaries, and performing some algebraic manipulation and simple integration, the final expression for gas rate is

$$q_g = \frac{2\pi khT_{sc}}{Tp_{sc}\ln(r_e/r_w)} \times \int_{p_{wf}}^{p_e} \frac{p}{\mu_g Z}\,dp. \tag{2.39}$$

Equations (2.38) and (2.39) presume that a set of consistent units has been used. Equation (2.39), written in field units for pseudosteady-state conditions, is

$$q_g = \frac{0.703kh}{T[\ln(r_e/r_w) - 0.75]} \times 2\int_{p_{wf}}^{p_R} \frac{p}{\mu_g Z}\,dp, \tag{2.40}$$

where terms and their units are: q_g (scf/D), k (md), h (ft), r (ft), T (°R), p (psia), and μ_g (cp). Standard conditions of 14.7 psia and 60°F (i.e., 520°R) are assumed in the constant 0.703, as is $Z = 1$ at standard conditions. The integral in equation (2.40) represents the area under the curve of $p/\mu_g Z$ versus pressure. Figure 2.10 shows a typical plot of the gas pressure function $p/\mu_g Z$.

The pressure function exhibits three distinct regions of behavior. At low pressures, usually less than 2000 psia, the $p/\mu_g Z$ curve is linear, and intercepts at the origin. This is equivalent to the observation that $1/\mu_g Z$ is essentially constant at low pressures (see fig. 2.11). At pressures higher than about 3000 psia the pressure function $p/\mu_g Z$ is nearly constant, showing some decrease at increasing pressures. Between 2000 and 3000 psia the pressure function shows distinct curvature. In review, the pressure function $p/\mu_g Z$ has three regions of behavior: low-pressure linearity, intermediate-pressure curvature, and high-pressure flattening. We might note that $p/\mu_g Z$ is directly proportional to $1/\mu_g B_g$, where $p/\mu_g Z = [p_{sc}(T/T_{sc})]$ $(1/\mu_g B_g)$.

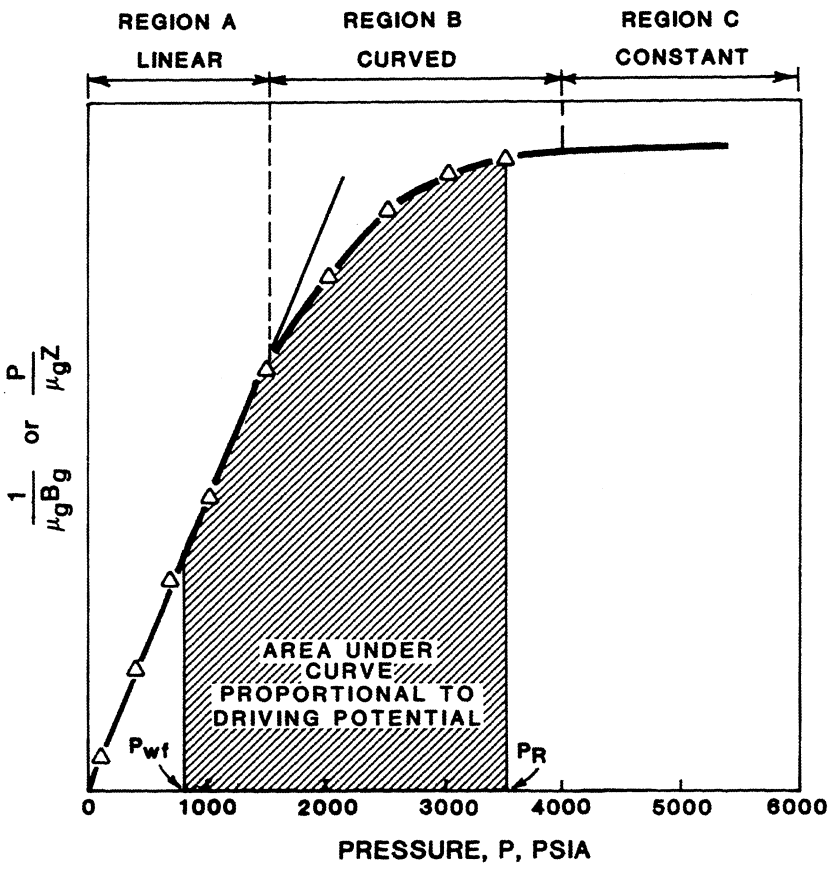

Figure 2.10 Gas pressure function.

The low-pressure behavior of $p/\mu_g Z$ results in a simple analytical solution to the pressure integral in equation (2.40):

$$2\int_{p_{wf}}^{p_R} \frac{p}{\mu_g Z}\,dp = \frac{p_R^2 - p_{wf}^2}{\mu_g Z}, \tag{2.41}$$

where p_R is assumed to be less than about 2000 psia. As indicated in figure 2.11, $1/\mu_g Z$ is essentially constant in the low-pressure region, and thus μ_g and Z can be evaluated at any pressure. By convention, we usually evaluate μ_g and Z at p_R. The radial flow equation for gas at *low pressures* can now be written

$$q_g = \frac{0.703\,kh(p_R^2 - p_{wf}^2)}{T\mu_g Z[\ln(r_e/r_w) - 0.75 + s]}, \tag{2.42}$$

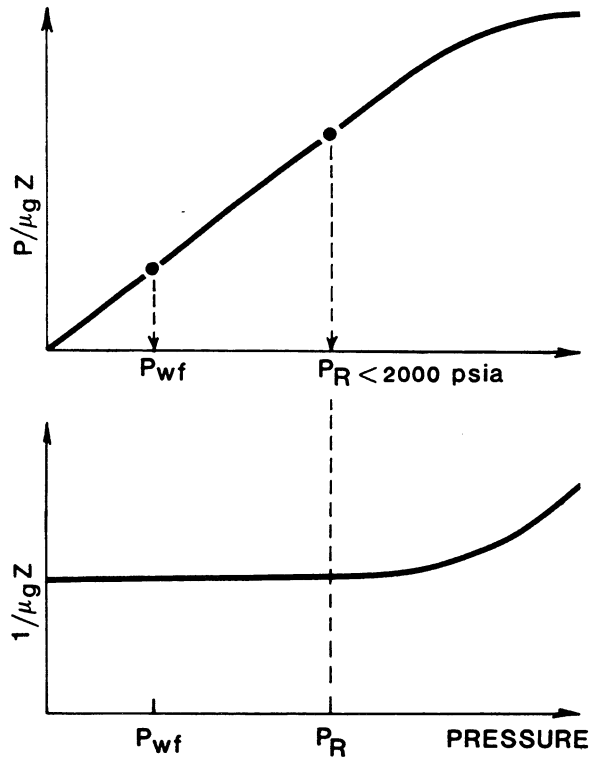

Figure 2.11 Low-pressure behavior of gas pressure function, $p/\mu_g Z$, and $1/\mu_g z$.

where skin s is defined as

$$s = \frac{0.703kh}{q_g T \mu_g Z}(p_{wf}'^2 - p_{wf}^2) \tag{2.43}$$

Recalling that p_{wf}' indicates wellbore flowing pressure for an ideal well, the skin factor in Equation (2.43) is proportional to delta pressure squared, caused by nonideal flow.

Using the Forchheimer modification to Darcy's law for high-velocity flow, equation (2.42) can be written

$$q_g = \frac{0.703kh(p_R^2 - p_{wf}^2)}{T\mu_g Z[\ln(r_e/r_w) - 0.75 + s + Dq_g]}, \tag{2.44}$$

where D is proportional to constant b in the Forchheimer equation (eq. [2.36]). The term Dq_g is commonly referred to as rate-dependent skin and is discussed in detail in section 3.4.

Although equations (2.42) and (2.44) appear similar except for the term Dq_g, they represent two different flow models. While the first one expresses the linear rate–pressure relationship of Darcy's law, the second one expresses the Forchheimer model. This similarity in form is very useful. It allows for all equations that are developed with Darcy's law to be modified to account for high-velocity effects by merely adding a rate-dependent skin term. Example 2.4 illustrates the use of the radial flow equation for gas wells producing at low reservoir pressures.

EXAMPLE 2.4 INFLOW PERFORMANCE CALCULATIONS FOR A GAS WELL PRODUCING AT LOW RESERVOIR PRESSURES

A two-rate drawdown/buildup test was run on a new gas discovery well in Kansas, the Medicine Lodge No. 1. For the first buildup following an eight-hour flow period at 6.4 MMscf/D, Horner analysis indicated a permeability-thickness (kh) of 790 md-ft and a skin of +3.62. The second buildup followed a 12-hour flow period at 8.7 MMscf/D, and Horner analysis indicated a kh of 815 md-ft and a skin of +4.63. Other reservoir data included initial reservoir pressure of 1623 psia at a temperature of 128°F. From standard gas property correlations, the initial gas viscosity and Z-factor are 0.0134 cp and 0.879, respectively.

Determine the high-velocity flow term D, used in the radial flow equation (2.44). What is the steady-state skin factor (i.e., when rate equals zero)? Write the IPR equation using the pressure-squared, low-reservoir pressure assumptions. Assume an average kh of 800 md-ft and $\ln(r_e/r_w) - 0.75 = 7$.

SOLUTION

First, we determine the rate-dependent skin coefficient D using skins reported from buildup test analysis. However, since a different kh is reported for each test, it is necessary to calculate an average kh and then correct the skin accordingly. Assuming stabilized flow, the corrected test skin s_{tc} is found from the actual test skin s_t from the relation

$$\frac{(kh)_{\text{test}}}{\ln(r_e/r_w) - 0.75 + s_t} = \frac{(kh)_{\text{avg}}}{\ln(r_e/r_w) - 0.75 + s_{tc}}$$

In this example we assume $\ln(r_e/r_w) - 0.75 = 7$ and $(kh)_{\text{avg}} = 800$ md-ft. The corrected test skin for the first test with rate of 6.4 MMscf/D is

$$\frac{790}{7 + 3.62} = \frac{800}{7 + s_{tc}}$$

or

$$s_{tc} = (800/790)(7 + 3.62) - 7$$

$$= 3.75.$$

EXAMPLE 2.4 continued

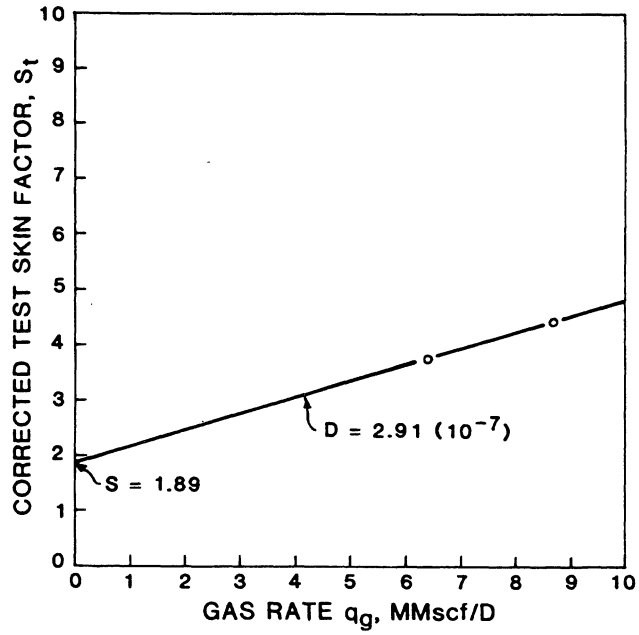

Figure E2.4a Rate-dependent skin factor in the Medicine Lodge No. 1 gas well.

For the second test with rate of 8.7 MMscf/D, corrected skin is

$$\frac{825}{7+4.63}=\frac{800}{7+s_{tc}}$$

or

$$s_{tc}=(800/815)(7+4.63)-7$$

$$=4.42.$$

A plot of corrected test skin versus gas rate is shown in figure E2.4a. The slope of the straight line gives a value of $D=2.91\times10^{-7}$ (scf/D)$^{-1}$. The intercept at zero rate equals the steady-state skin, $s=+1.89$, indicating slight formation damage.

A common error is to plot test skin versus rate without making the kh correction. Had this been done for this example the steady-state skin would be underestimated, rate-dependent skin would be overestimated, and AOF would be underestimated by 1.0 MMscf/D (corresponding to about $700,000 per year for a gas price of $2/Mscf). *It must be emphasized that the skin-versus-rate plot is not valid if kh associated with each skin is different.*

EXAMPLE 2.4 continued

Table E2.4 Calculated Gas IPR for the Medicine Lodge No. 1 Well

p_{wf} (psia)	$p_R^2 - p_{wf}^2$ (psia^2)	q_g (MMscf/D)
0	2.63×10^6	15.8 (AOF)
500	2.38×10^6	14.7
750	2.07×10^6	13.2
1000	1.63×10^6	11.0
1250	1.07×10^6	7.78
1500	3.84×10^5	3.18
1550	2.32×10^5	1.99

The stabilized IPR equation for the Medicine Lodge No. 1 is found by substituting reservoir and test data in equation (2.44).

$$q_g = \frac{0.703(800)(1623^2 - p_{wf}^2)}{(128+460)(0.0134)(0.879)[7 + 1.89 + 2.91 \times 10^{-7} q_g]}$$

$$= 81.2 \frac{(2.63 \times 10^6 - p_{wf}^2)}{(8.89 + 2.91 \times 10^{-7} q_g)}$$

or

$$\frac{2.63 \times 10^6 - p_{wf}^2}{q_g} = 0.1095 + 3.58 \times 10^{-9} q_g,$$

giving $A = 0.1095$ and $B = 3.58 \times 10^{-9}$. Solving the quadratic equation for rate,

$$Bq_g^2 + Aq_g - \Delta p^2 = 0$$

$$q_g = \frac{[A^2 + 4B\Delta p^2]^{0.5} - A}{2B}$$

$$= \frac{[(0.1095)^2 + 4(3.58 \times 10^{-9})(2.63 \times 10^6 - p_{wf}^2)]^{0.5} - 0.1095}{2(3.58 \times 10^{-9})}$$

$$= \frac{[0.0120 + 1.43 \times 10^{-8}(2.63 \times 10^6 - p_{wf}^2)]^{0.5} - 0.1095}{7.16 \times 10^{-9}}.$$

Table E2.4 gives a few rates and flowing pressures, which are plotted in figure E2.4b on log–log paper. From about 5 MMscf/D to the maximum rate (AOF) of 16 MMscf/D, the IPR curve is a straight line on the log–log plot. The slope is 1.89, corresponding to a backpressure exponent of $n = 0.766$.

EXAMPLE 2.4 continued

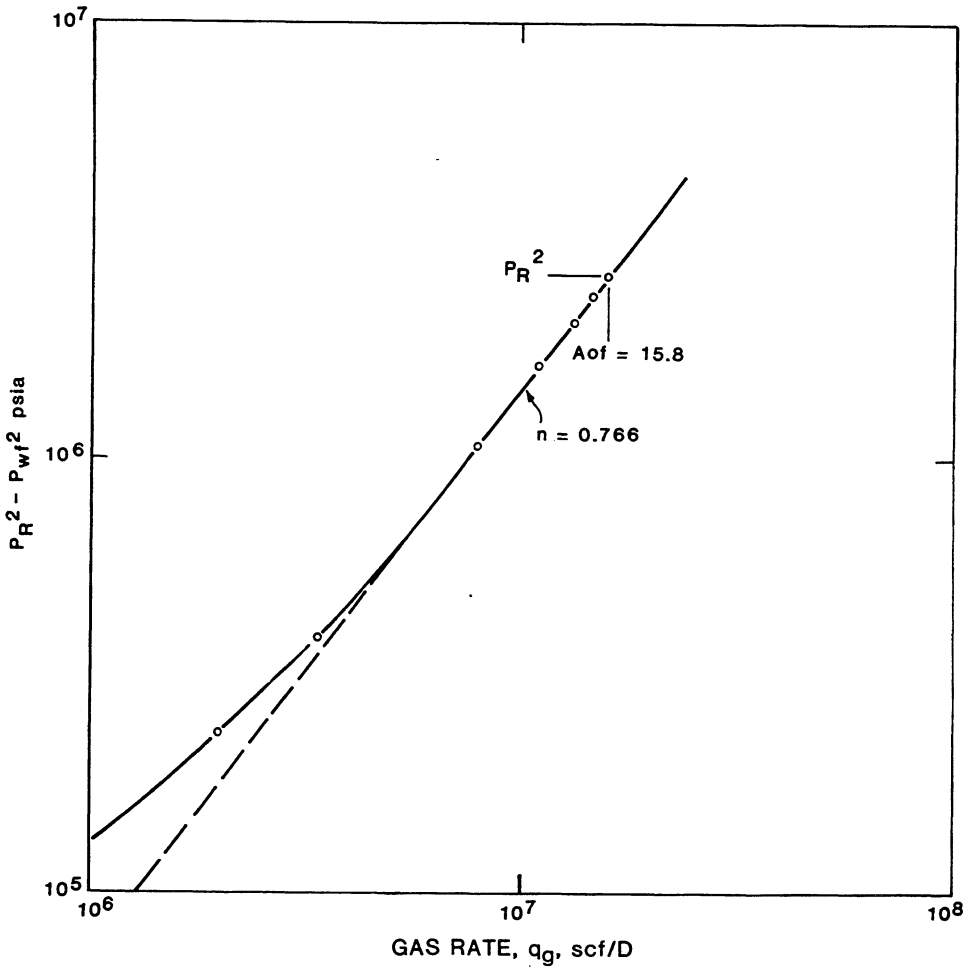

Figure E2.4b Backpressure curve of the Medicine Lodge No. 1 gas well.

At high pressures, usually greater than 3000 to 3500 psia, the pressure function $p/\mu_g Z$ is nearly constant. The pressure integral in equation (2.40) is solved analytically to give

$$2\int_{p_{wf}}^{p_R} \frac{p}{\mu_g Z}\,dp = 2\frac{p}{\mu_g Z}(p_R - p_{wf}), \tag{2.45}$$

where $p/\mu_g Z$ is evaluated at any pressure between p_{wf} and p_R, although we must emphasize that *both* pressures must be higher than about 3000 psia. The resulting IPR equation for gas wells producing at high flowing and static pressures is

$$q_g = \frac{1.406kh(p/\mu_g Z)(p_R - p_{wf})}{T[\ln(r_e/r_w) - 0.75 + s + Dq_g]}. \tag{2.46}$$

The high-pressure approximation of gaswell IPR is not commonly used by engineers. We mention it only to bring attention to the similarity between high-pressure gas and undersaturated oil flow.

The pressure-squared approach for low-pressure gas wells and the straight-line IPR for high-pressure gas wells are only valid in the regions of pressure for which they are designed. A more general approach to account for the pressure dependence of gas properties is to perform the integration of $p/\mu_g Z$ (eq. [2.40]) for the entire range of pressures applicable to a given well. This amounts to calculating the area under the $p/\mu_g Z$ curve from p_{wf} to p_R.

Figure 2.12 illustrates a useful property of integration that is applied to solve the integral in practical engineering problems. Let us define the area from zero pressure (vacuum) to any other pressure as $A(p)$. It can be shown that the area under the $p/\mu g Z$ curve from p_1 to p_2 is merely $A(p_2) - A(p_1)$, where $p_2 > p_1$. A special name, pseudopressure, designated $m(p)$, has been given to the quantity $2A(p)$ (Al-Hussainy, et. al. 1966). That is,

$$m(p) = 2\int_0^p (p/\mu_g Z)dp, \tag{2.47}$$

where $m(p)$ is the analog to pressure or pressure squared in equation (2.41). The differential pseudopressure, $\Delta m(p) = m(p_R) - m(p_{wf})$, represents the driving force or potential moving gas toward the well. Mathematically, $\Delta m(p)$ is given by

$$\begin{aligned}\Delta m(p) &= 2\int_{p_{wf}}^{p_R} (p/\mu_g Z)dp \\ &= 2\int_0^{p_R} (p/\mu_g Z)dp - 2\int_0^{p_{wf}} (p/\mu_g Z)dp = m(p_R) - m(p_{wf}).\end{aligned} \tag{2.48}$$

Substituting equation (2.48) in the radial flow equation (eq. [2.40]) and including the effect of high-velocity flow, the most general gas IPR for stabilized flow is

$$q_g = \frac{0.703kh[m(p_R) - m(p_{wf})]}{T[\ln(r_e/r_w) - 0.75 + s + Dq_g]}. \tag{2.49}$$

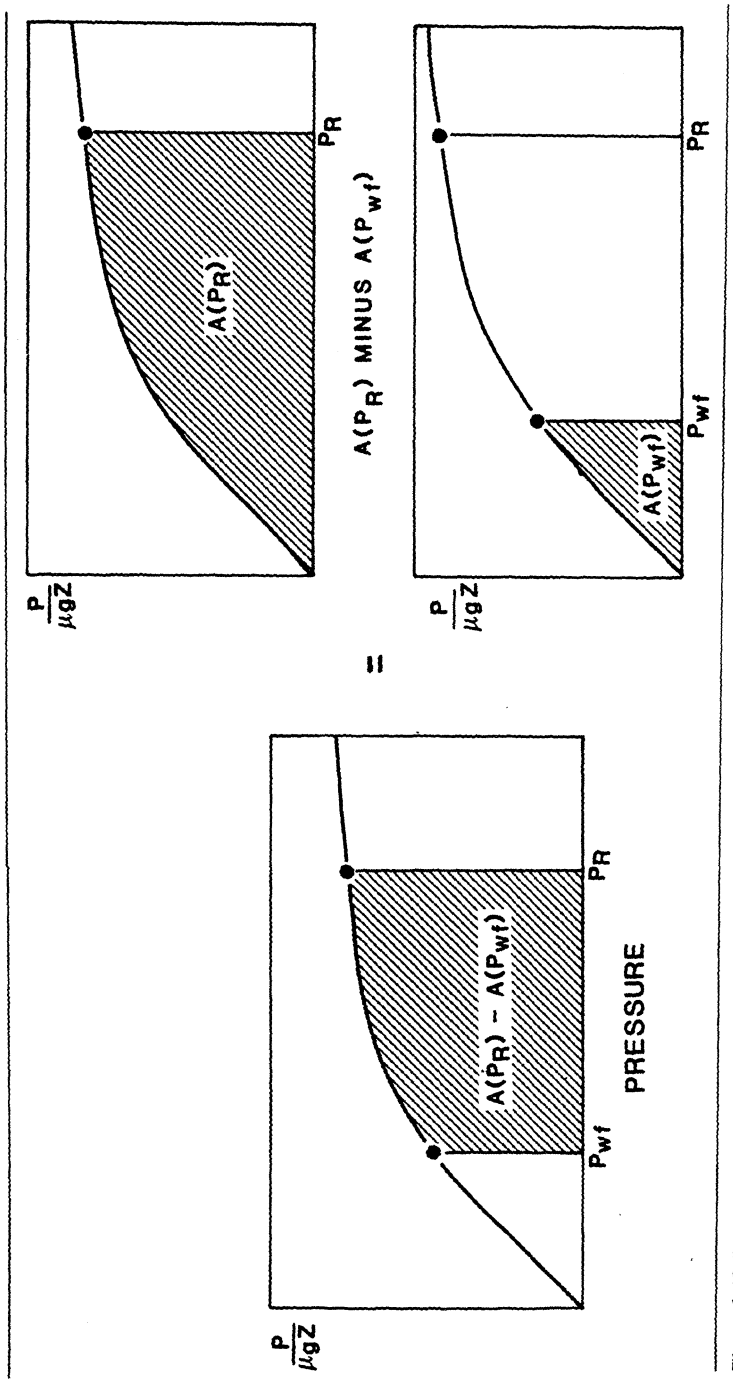

Figure 2.12 Useful property of integration shown graphically and used by the pseudopressure approach.

The relation for skin is then written

$$s = \frac{0.703kh}{q_g T}[m(p_{wf}') - m(p_{wf})], \tag{2.50}$$

where $m(p_{wf}')$ corresponds to the ideal wellbore flowing pressure p_{wf}', and $m(p_{wf})$ corresponds to the actual (nonzero skin) flowing pressure p_{wf}.

Two practical problems are usually associated with the pseudopressure function $m(p)$: (1) It must be calculated by tabulating p, μ, and Z, plotting $p/\mu Z$, and integrating graphically or numerically. (2) The magnitude of $m(p)$ is much larger than pressure (usually on the order of 100 times pressure-squared, or $m[p] \approx 100p^2$). These problems can be overcome with some practice, as is shown in example 2.5.

EXAMPLE 2.5 CALCULATING THE GAS PSEUDOPRESSURE FUNCTION $m(p)$

This example shows a simple procedure for calculating the gas pseudopressure function $m(p)$. The integral in equation (2.47) can usually be approximated with sufficient accuracy from the trapezoid rule of integration. This is perhaps best illustrated by a simple procedure summarized in table E2.5. Each step corresponds to a column in the table.

Basic Data:

[1] p : pressure (psia)
[2] Z : gas compressibility factor
[3] μ_g : gas viscosity (cp)

Calculate:

[4] $p/\mu_g Z$: pressure function (psia/cp)
[5] $(p/\mu_g Z)_{av}$: average for two successive entries (psia/cp)
[6] Δp : pressure difference for two successive entries (psi)
[7] $2(p/\mu_g Z)_{av}\Delta p$: incremental pseudopressure (psi^2/cp)
[8] $m(p)$: the sum of products in column (7) (psi^2/cp)

Table E2.5 tabulates the eight quantities. The calculated pseudopressure function is plotted in figure E2.5.

EXAMPLE 2.5 continued

Table E2.5 Calculation Procedure for Gas Pseudopressure, $m(p)$

p [1]	Z [2]	μ_g [3]	$p/\mu_g Z$ [4]	$(p/\mu_g Z)_{av}$ [5]	Δp [6]	2([5][6]) [7]	$m(p)$ = Sum [7] [8]
0			0				
14.7	0.998	0.0127	1,160	580[a]	14.7	1.70 E4[b]	1.70 E4
400	0.960	0.0130	32,051	16,606	385	1.28 E7	1.28 E7
800	0.925	0.0135	64,064	48,058	400	3.84 E7	5.12 E7
1200	0.895	0.0143	93,761	78,913	400	6.31 E7	1.14 E8
1600	0.873	0.0152	120,576	107,169	400	8.57 E7	2.00 E8
2000	0.860	0.0162	143,554	132,065	400	1.06 E8	3.06 E8
2250	0.856	0.0169	155,533	149,544	250	7.48 E7	3.81 E8
2500	0.857	0.0177	164,811	160,172	250	8.01 E7	4.61 E8
2750	0.860	0.0185	172,847	168,829	250	8.44 E7	5.45 E8
3000	0.867	0.0193	179,285	176,066	250	8.80 E7	6.33 E8
3150	0.872	0.0197	183,370	181,328	150	5.44 E7	6.88 E8

[a]Column [5] lists the arithmetic average of the pressure function $p/\mu_g Z$ in the pressure interval Δp.
[b]1.70 E4 is the notation for 1.70×10^4.

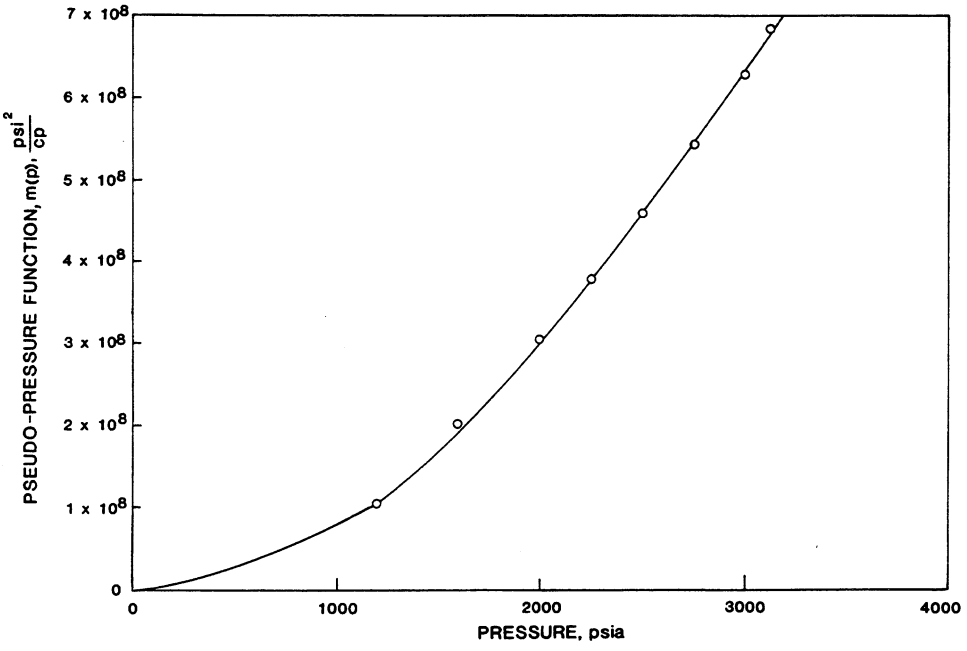

Figure E2.5 Pseudopressure function versus pressure.

An important characteristic of the pseudopressure function is that it is only necessary to calculate gas pseudopressure one time for a given field. Afterwards, it can apply to all wells in a gas field throughout the production life. Example 2.6 illustrates the use of the pseudopressure function to predict the IPR of a gas well.

EXAMPLE 2.6 GAS IPR CALCULATED USING PRESSURE-SQUARED AND PSEUDOPRESSURE METHODS

The 0.61-gravity gas considered in example 2.5 applies to the Crawford gas reservoir in northwestern Nebraska. The Crawford No. 1 produces from the Mississippi Chat at a depth of about 7040 ft. Initial reservoir pressure was 3150 psia, and the maximum temperature recorded during the well test was 148°F. The SP, gamma ray, and induction logs indicate a net pay of about 22 ft. The Chat is a clean sand with similar quality throughout the Crawford field, and usually requiries a small acid treatment to remove formation damage. Core and test permeabilities for the No. 1 well averaged about 20 md. Local graduate students from a state university studied the effect of high-velocity flow on several Chat core samples. They correlated high-velocity coefficient and permeability data and concluded that a D term of 1.5×10^{-6} 1/scf/D could be used for the Crawford No. 1 well.

The well could not be tested at high rates because no pipeline hookup was available and the No. 1 well was located on the edge of the Crawford city limits, in a residential area. Before drilling more wells, the operator requests an estimation of the well's deliverability. Make the following calculations using (a) the pressure-squared gas IPR (eq. [2.44]) and (b) the pseudopressure gas IPR.

1. Calculate and plot the gas IPR on Cartesian paper.
2. Determine the AOF.

SOLUTION

Since the spacing and estimated drainage area are not known, $\ln(r_e/r_w) - 0.75$ will be assumed equal to 7.0. Since the formation sand face has been cleaned with acid, steady-state skin of zero is assumed. Using the available rock and fluid properties the two IPR equations are

$$q_g = \frac{0.703(20)(22)(3150^2 - p_{wf}^2)}{(148 + 460)(0.0197)(0.872)(7 + 1.5 \times 10^{-6} q_g)}$$

$$= 29.6(9.92 \times 10^6 - p_{wf}^2)/(7 + 1.5 \times 10^{-6} q_g)$$

or, when rearranged

$$\frac{9.92 \times 10^6 - p_{wf}^2}{q_g} = A + Bq_g$$

$$= 0.236 + 5.07 \times 10^{-8} q_g,$$

EXAMPLE 2.6 continued

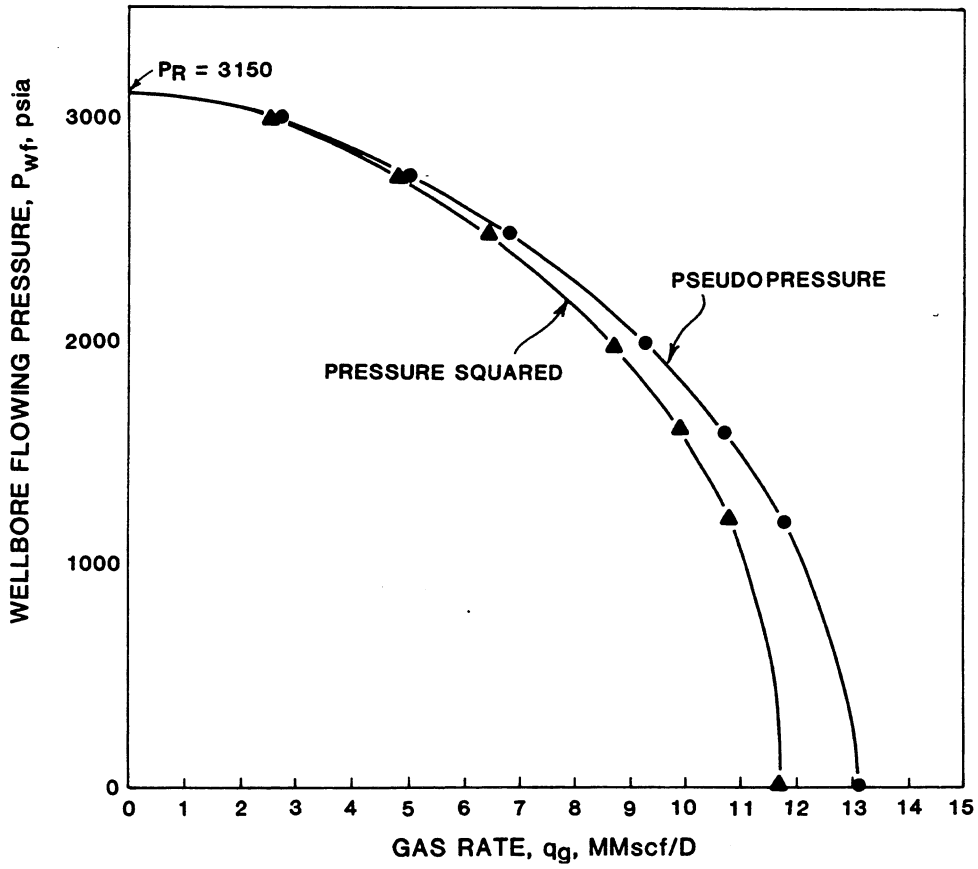

Figure E2.6 IPR curves of the Crawford No. 1 gas well using pseudopressure and pressure-squared approaches.

yielding the q_g solution

$$q_g = \frac{[A^2 + 4B\Delta p^2]^{0.5} - A}{2B}$$

$$= \frac{[0.0557 + 2.03 \times 10^{-7}(9.92 \times 10^6 - p_{wf}{}^2)]^{0.5} - 0.236}{1.01 \times 10^{-7}}.$$

Using the pseudopressure IPR, gas rate is expressed by

$$q_g = \frac{0.703(20)(22)[6.88 \times 10^8 - m(p_{wf})]}{(148 + 460)(7 + 1.5 \times 10^{-6} q_g)}$$

$$= 0.509[6.88 \times 10^8 - m(p_{wf})]/(7 + 1.5 \times 10^{-6} q_g)$$

EXAMPLE 2.6 continued

Table E2.6 Calculation of Gas IPR Curves for the Crawford No. 1 Well

			q_g (MMscf/D) for IPR	
p_{wf} (psia)	p_{wf}^2 (psia^2)	$m(p_{wf})$ (psi^2/cp)	PRESSURE-SQUARED	PSEUDO-PRESSURE
0	0.00	0.00	11.7	13.1
1200	1.44 E6	1.14 E8	10.8	11.8
1600	2.56 E6	2.00 E8	9.96	10.7
2000	4.00 E6	3.06 E8	8.74	9.28
2500	6.25 E6	4.61 E8	6.50	6.74
2750	7.56 E6	5.45 E8	4.89	5.01
3000	9.00 E6	6.33 E8	2.53	2.57

or by the quadratic equation with $A = 13.8$ and $B = 2.95 \times 10^{-6}$ with the direct solution

$$q_g = \frac{[190 + 1.18 \times 10^{-5}[6.88 \times 10^8 - m(p_{wf})]^{0.5} - 13.8}{5.90 \times 10^{-6}}.$$

Table E2.6 tabulates the results of the calculations needed to plot the two IPR curves as in figure E2.6. The plot indicates that IPR calculated by the pressure-squared approach is more conservative than IPR calculated by the pseudopressure approach.

Concerning the practical application of the radial flow equation including rate-dependent skin Dq_g, equation (2.44) can also be written as a quadratic equation (Forchheimer model)

$$p_R^2 - p_{wf}^2 = Aq_g + Bq_g^2, \tag{2.51}$$

where

$$A = \frac{T\mu_g Z}{0.703kh}[\ln(r_e/r_w) - 0.75 + s] \tag{2.52}$$

and

$$B = \frac{T\mu_g Z}{0.703kh} D. \tag{2.53}$$

The term $\mu_g Z$ can be evaluated at any pressure as long as $p_R < 2000$ psia.

For high-pressure gas wells with limited drawdown, pressure can be used instead of pressure-squared, in which case the Forchheimer quadratic equation is written

$$p_R - p_{wf} = Aq_g + Bq_g^2, \tag{2.54}$$

where

$$A = \frac{T}{1.407kh}\left(\frac{\mu_g Z}{p_{av}}\right)[\ln(r_e/r_w) - 0.75 + s] \tag{2.55}$$

and

$$B = \frac{T}{1.407kh}\left(\frac{\mu_g Z}{p_{av}}\right)D. \tag{2.56}$$

Note that $\mu_g Z$ is evaluated at $p_{av} = (p_R + p_{wf})/2$.

If pseudopressure $m(p)$ is used instead of pressure-squared, the rate equation is written

$$m(p_R) - m(p_{wf}) = Aq_g + Bq_g^2, \tag{2.57}$$

where

$$A = \frac{T}{0.703kh}[\ln(r_e/r_w) - 0.75 + s] \tag{2.58}$$

and

$$B = \frac{T}{0.703kh}D. \tag{2.59}$$

The most practical solution of the Forchheimer equation is to plot $(p_R^2 - p_{wf}^2)/q_g$ versus q_g, $(p_R - p_{wf})/q_g$ versus q_g, or $[m(p_R) - m(p_{wf})]/q_g$ versus q_g on linear coordinate paper. The result is a straight line with intercept A and slope B. Figure 2.13 illustrates such a plot, using pressure-squared for a low-pressure gas well. The slope B in figure 2.13 indicates the significance of high-velocity effect on the productivity of the well. A large slope implies large rate-dependent skin. The intercept A is related to steady-state skin factor.

If rate needs to be written in terms of flowing pressure, the quadratic equations can be solved as follows:

$$q_g = \frac{[A^2 + 4B\Delta p^2]^{0.5} - A}{2B}, \tag{2.60}$$

$$q_g = \frac{[A^2 + 4B\Delta p]^{0.5} - A}{2B}, \tag{2.61}$$

and

$$q_g = \frac{[A^2 + 4B\Delta m(p)]^{0.5} - A}{2B}, \tag{2.62}$$

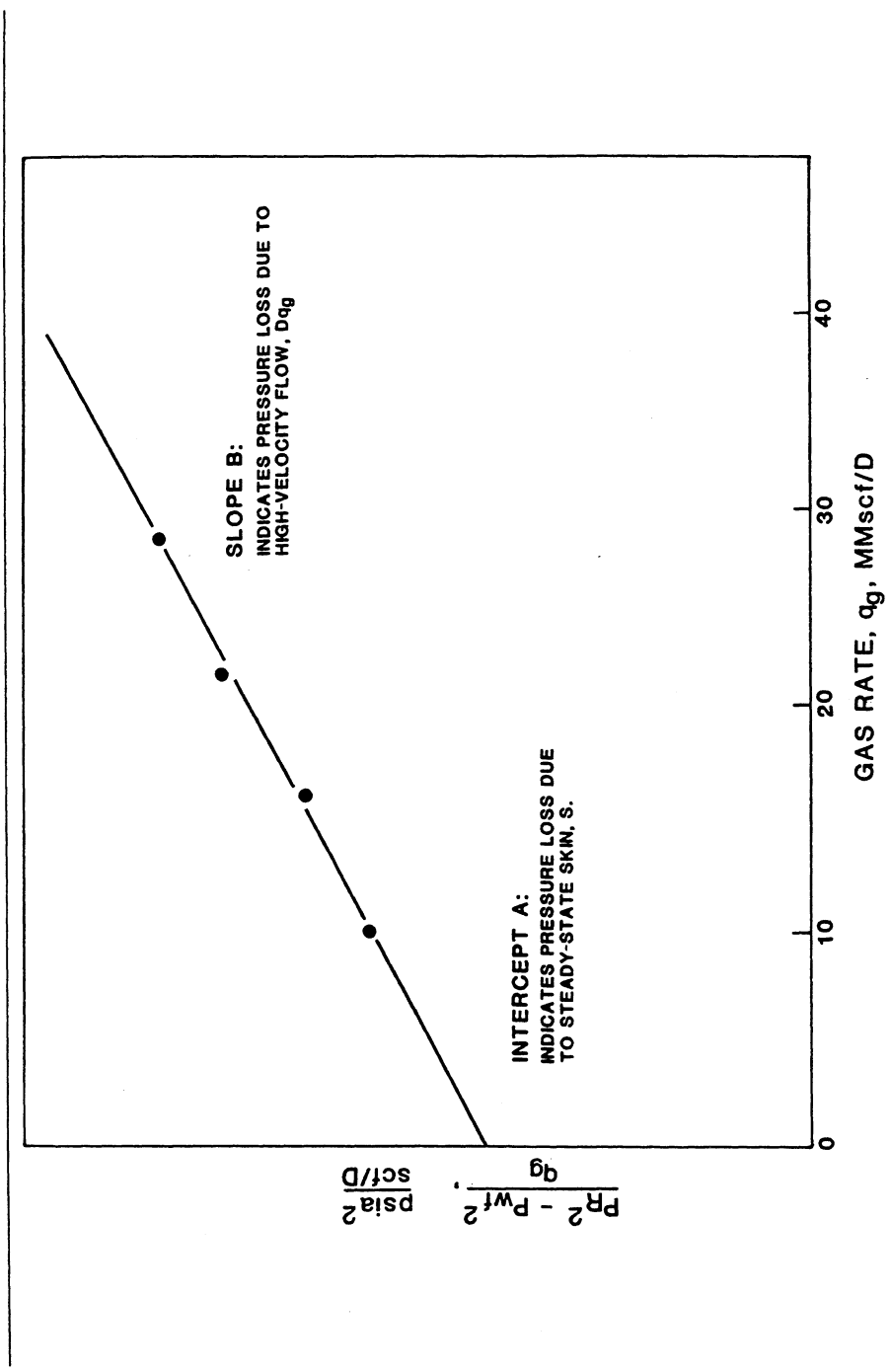

Figure 2.13 Linear plot for determining high-velocity flow effect on well performance.

where $\Delta p^2 = p_R^2 - p_{wf}^2$, $\Delta p = p_R - p_{wf}$, and $\Delta m(p) = m(p_R) - m(p_{wf})$. Obviously, values of A and B will be different, depending on whether pressure, pressure-squared, or pseudopressure is used.

Example 2.7 illustrates the linearized plot of test data for a gas well. The constant D in the rate dependent skin factor is related to the slope B of the linear plot in figure 2.13 by equations (2.53), (2.56), or (2.59). By combining equations (2.37) and (2.44) the constant is related also to rock properties,

$$D = 2.222 \times 10^{-18} \frac{\gamma_g kh}{\mu_g r_w h_p^2} \beta. \tag{2.63}$$

EXAMPLE 2.7 LINEAR PLOT OF GASWELL TEST DATA

The Cullender No. 5 gas well produces from a shallow, low-pressure, highly productive reservoir. The well has been tested by a multirate test and the results are listed in table E2.7. One-hour duration of each flow period was enough to reach stabilization of flowing wellbore pressure. In fact, it was observed that pressures stabilized almost instantaneously after each rate change.

The three high flow rates (March 30, 1950) were obtained by flow-after-flow sequence without shut-in between flow periods. The three low flow rates were performed at three consecutive days; each flow period started from shut-in conditions. Determine the IPR and evaluate the high-velocity-flow effects in the well.

SOLUTION

The reservoir did not exhibit appreciable depletion during the test period and reservoir pressure was essentially constant. Downhole pressures listed in table E2.7 were calculated from wellhead pressures using vertical flow correlations, which probably explains the spread in static reservoir pressures. The IPR will be established by using both the backpressure equation and the quadratic equation.

The log–log backpressure plot in figure E2.7a gives a straight line which defines a backpressure exponent $n = 1/\text{slope} = 0.55$. The backpressure coefficient is calculated from the curve as

$$C = 8.737 \times 10^6/(11270)^{0.55} = 49{,}468 \text{ scf/D/psi}^2.$$

The backpressure equation then is

$$q_g = 49{,}468(p_R^2 - p_{wf}^2)^{0.55},$$

and the absolute open-flow is 39.8 MMscf/D.

A Cartesian plot of $\Delta p^2/q_g$ versus q_g (fig. E2.7b) gives a straight line (except for a small deviation and the low-rate point). The intercept of the line is

EXAMPLE 2.7 continued

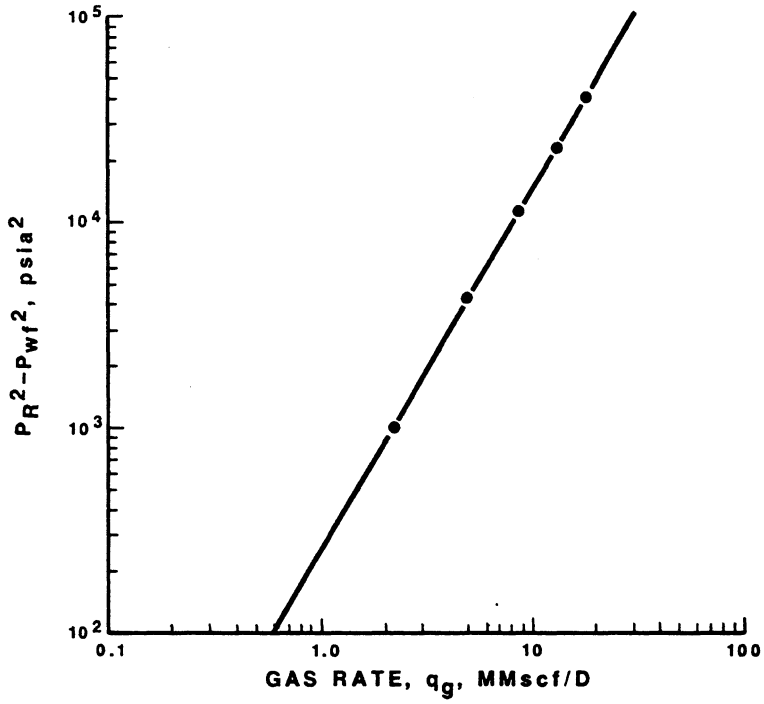

Figure E2.7a Stabilized backpressure curve of the Cullender No. 5 gas well. Reprinted by permission of the SPE-AIME from Cullender 1955. © 1955 SPE-AIME.

$$A = 0.00028 \frac{\text{psia}^2}{\text{scf/D}}.$$

The slope is

$$B = 1.26 \times 10^{-4} \frac{\text{psia}^2/\text{scf/D}}{\text{MMscf/D}}$$

or, when expressed in scf/D,

$$B = 1.26 \times 10^{-10} \frac{\text{psia}^2/\text{scf/D}}{\text{scf/D}}.$$

The low n value and the high B value indicate large rate-dependent skin.

Reservoir data were not presented by Cullender (1955) and it is therefore difficult to quantify steady-state skin s and rate-dependent skin coefficient D. It is certain, however, that rate-dependent pressure losses dictate reservoir inflow performance.

EXAMPLE 2.7 continued

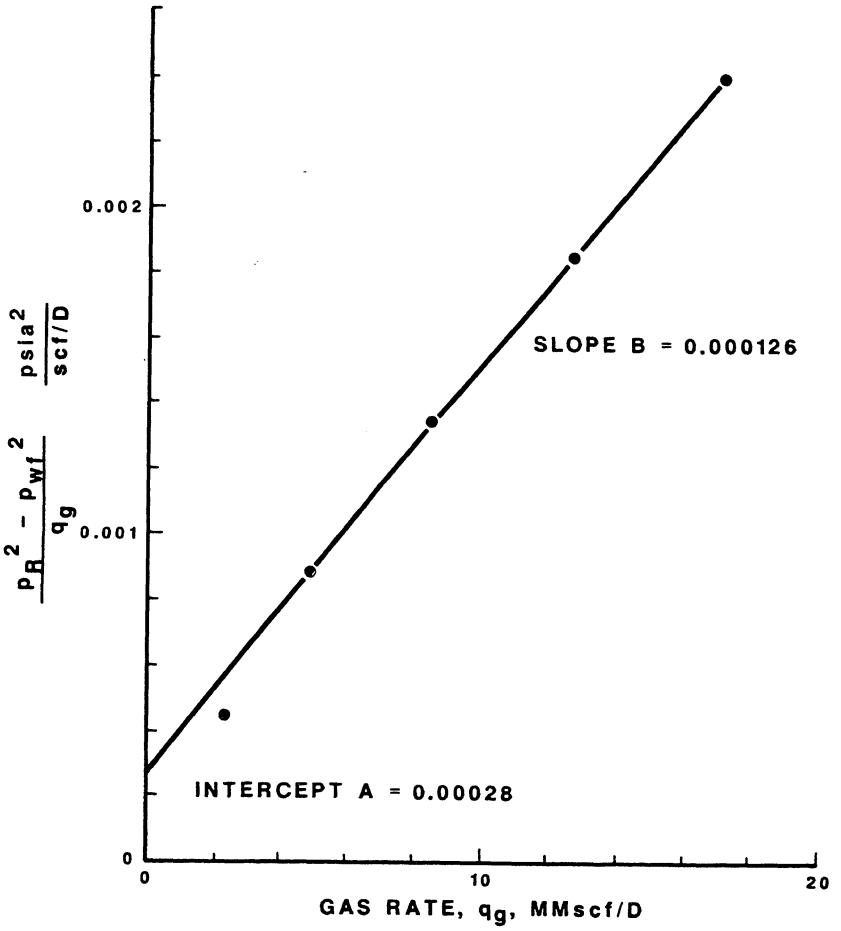

Figure E2.7b Stabilized quadratic IPR curve of the Cullender No. 5 gas well.

Table E2.7 Test Data of Cullender No. 5 Gas Well (March–April 1950)

Date	p_R psia	Δt hr	p_{wf} psia	q_g MMscf/D	$p_R^2 - p_{wf}^2$ psia^2	$\Delta p^2/q_g$ psia^2/scf/D
March 30	439.0	1	425.97	8.373	11270	0.001340
March 30	439.0	1	411.69	12.484	25250	0.001860
March 30	439.0	1	390.08	16.817	40600	0.002410
April 3	439.9	1	439.80	0.570	90	0.000158
April 4	439.6	1	438.45	2.231	1010	0.000453
April 5	439.8	1	434.86	4.841	4320	0.000892

The high velocity coefficient β (1/ft) can be approximated by an empirical correlation (discussed later in section 3.4)

$$\beta = 2.73 \times 10^{10} k_a^{-1.1045}, \tag{2.64}$$

where k_a is the permeability used to evaluate β, equal to the effective gas permeability near the wellbore. In equation (2.63), h_p is the formation thickness open to flow. If the near-wellbore region is not damaged or stimulated with acid, the D term is essentially independent of permeability, since β is approximately proportional to $1/k$ and D is proportional to βk. Without an estimate of permeability, D can be written (with $\beta \approx 1.69 \times 10^{10}/k$):

$$D = 3.75 \times 10^{-8} \frac{\gamma_g h}{\mu_g r_w h_p^2}. \tag{2.65}$$

The slope and intercept of the cartesian plot together with equations (2.63) and (2.49) provide a useful mean for interpreting multirate well test data in terms of formation properties and well completion data. Example 2.8 applies the quadratic rate equation to interpret test data.

EXAMPLE 2.8 HIGH-PRESSURE GASWELL MULTIRATE TEST INTERPRETATION

The McLeod No. 1A (McLeod 1983) is a high-pressure gas well producing from the Worth sandstone. During the first year of production, the average reservoir pressure dropped from 12,315 psia to 5,565 psia. Six tests have been run and relevant data are given in table E2.8a. General reservoir and well data are given in table E2.8b.

Use the quadratic equation to develop an inflow performance relation for the McLeod No. 1A at pressures encountered during the second year of production (approximately 5000 psia average reservoir pressure).

Table E2.8a Test Data for the McLeod No. 1A Well

	1	2	3	4	5	6
q_g (MMscf/D)	7.152	8.080	7.739	5.178	4.850	4.895
p_R (psia)	12,315	10,177	8,625	6,365	5,815	5,565
p_{wf}* (psia)	11,458	9,070	7,691	5,915	5,260	5,082
p_{av} (psia)	11,887	9,624	8,158	6,140	5,538	5,324
Z at p_{av}	1.55	1.38	1.26	1.10	1.05	1.04
μ (cp) at p_{av}	0.0380	0.0340	0.0310	0.0265	0.0245	0.0240
$(\Delta p/q_g)(p_{av}/\mu Z)$	24.2	28.1	25.2	18.3	24.6	21.0

*Bottomhole pressures calculated from surface pressures.

EXAMPLE 2.8 continued

Table E2.8b Reservoir and Well Data for the McLeod No. 1A Well

Formation permeability* k	200 md
Net pay h	26 ft
Estimated drainage radius r_e	1320 ft
Wellbore radius r_w	0.375 ft
Gas gravity γ_g	0.635
Formation temperature T_R	245°F

*From sidewall core data.

SOLUTION

The quadratic equation (2.51) can be written

$$\left(\frac{p_R - p_{wf}}{q_g}\right)\left(\frac{p_{av}}{\mu_g Z}\right) = A' + B'q_g,$$

where

$$A' = \frac{T}{1.407kh}[\ln(r_e/r_w) - 0.75 + s]$$

and

$$B' = \frac{T}{1.407kh}D.$$

Note that μ_g and Z are evaluated at p_{av}, where

$$p_{av} = (p_R + p_{wf})/2.$$

This form of normalizing pressure accounts for severe depletion and large changes in pressure-dependent properties during the period of testing. In other words, since the term $p_{av}/\mu_g Z$ shows considerable variation as a result of depletion, it has been eliminated from the expressions of the slope and the intercept. A plot of $[(\Delta p/q_g)(p_{av}/\mu_g Z)]$ versus q_g is shown in figure E2.8.

The reservoir has high permeability and the drainage volume appears to be limited, based on the rapid depletion indicated by the test data in table E2.8a. We can assume stabilized flow for all five tests. Two interpretations of the data are possible.

The first interpretation uses rates 1, 2, 3, and 4, which define a straight line with slope $B' = 3.01 \times 10^{-6}$ and intercept $A' = 2.7$. Based on $kh = 200(26) = 5200$ md-ft and $\ln(r_e/r_w) - 0.75 = \ln(1320/0.375) - 0.75 = 7.42$, we calculate

$$D = B'1.407kh/T$$

$$= 3.01 \times 10^{-6}(1.407)(5200)/(460 + 245)$$

EXAMPLE 2.8 continued

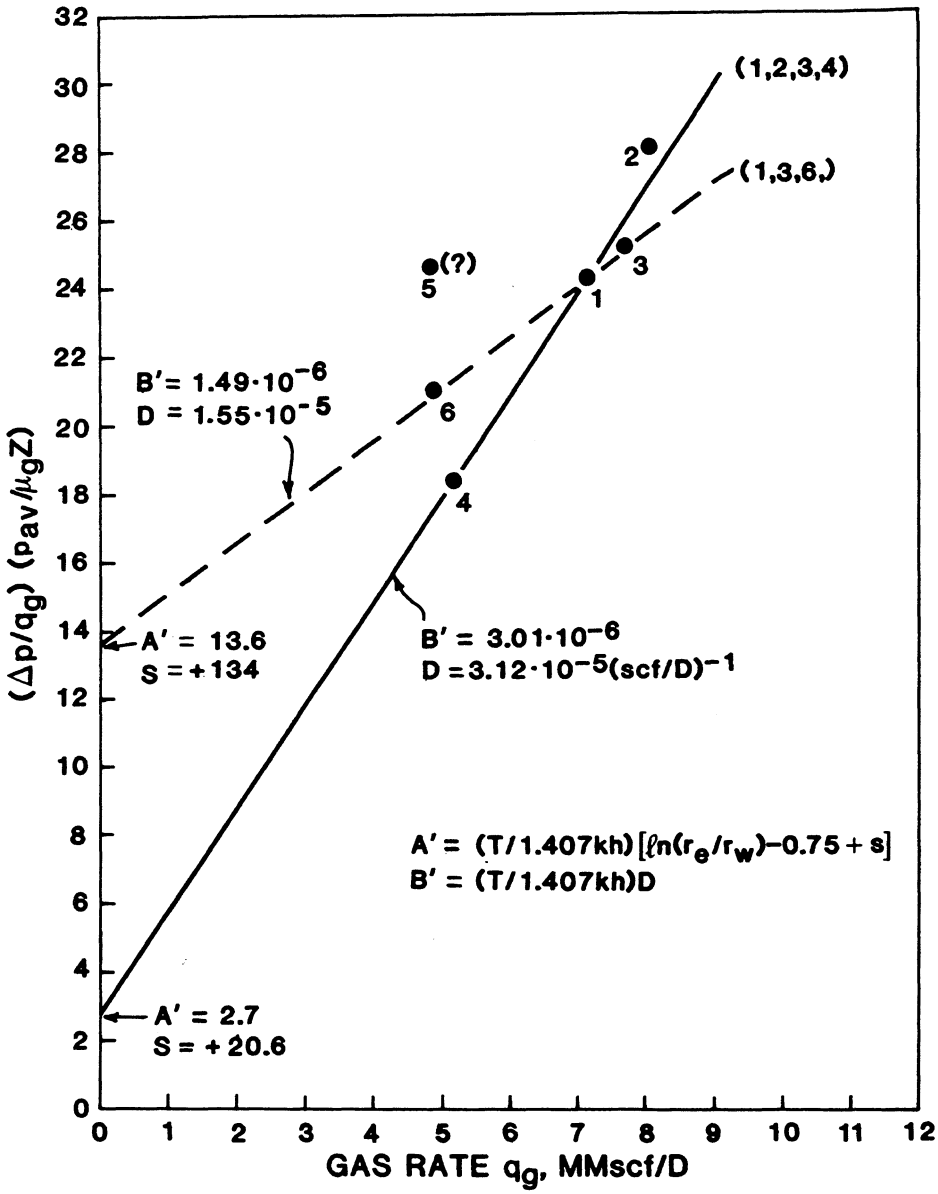

Figure E2.8 Quadratic IPR plot of test data of the McLeod No. 1 gas well.

EXAMPLE 2.8 continued

$$= 3.12 \times 10^{-5}(\text{scf/D})^{-1}$$

and

$$s = A' 1.407kh/T - [\ln(r_e/r_w) - 0.75]$$

$$= 2.7(1.407)(5200)/(460 + 245) - 7.42$$

$$= +20.6.$$

The second interpretation uses rates 1, 3, and 6 to define a straight line with slope $B' = 1.49 \times 10^{-6}$ and intercept $A' = 13.6$, yielding

$$D = 1.49 \times 10^{-6}(1.407)(5200)/(460 + 245)$$

$$= 1.55 \times 10^{-5}(\text{scf/D})^{-1}$$

and

$$s = 13.6(1.407)(5200)/(460 + 245) - 8.2$$

$$= +134.$$

The two interpretations are considerably different. Table E2.8c indicates the actual difference and its impact on stabilized well performance.

The conclusion about the test data is that (1) a damaged zone appears to restrict flow near the wellbore, and (2) the high-velocity flow is exacerbated by the damaged permeability. Also, the test data show considerable scatter, indicating changing conditions near the wellbore through the first year of production, and/or bad data. Part of the scatter may result from calculating bottomhole pressures from wellhead measurements. McLeod used the test data to substantiate a high-velocity-flow model for the perforations. His model is discussed in chapter 3 (section 3.5) and in example 3.8.

Table E2.8c Results of Two Interpretations of Test Data for the McLeod No. 1A

	Total Skin $s + Dq$ (well flowing pressure)	
(MMscf/D)	$s = +20.6$, $D = 3.12 \times 10^{-5}$	$s = +134$, $D = 1.55 \times 10^{-5}$
2	82.2 (4921)*	164.0 (4849)
4	144.6 (4732)	195.0 (4644)
6	207.0 (4434)	226.0 (4384)
8	269.4 (4027)	257.0 (4071)
10	331.8 (3511)	288.0 (3703)

*$p_R = 5000$ psia, $(p_{av}/\mu_g Z) = 220{,}000$, or $1/\mu_g Z = 0.0227\ cp^{-1}$.

Comparing equation (2.42) with the backpressure equation, we can write an expression for C (stabilized) in terms of reservoir properties for the case of $n = 1$:

$$q_g = C(p_R^2 - p_{wf}^2), \tag{2.66}$$

where

$$C = \frac{0.703kh}{T\mu_g Z[\ln(r_e/r_w) - 0.75 + s]}. \tag{2.67}$$

When applied for a high-pressure gas well,

$$q_g = C(p_R - p_{wf}), \tag{2.68}$$

where

$$C = \frac{1.407p_{av}kh}{T\mu_g Z[\ln(r_e/r_w) - 0.75 + s]}, \tag{2.69}$$

with $\mu_g Z$ evaluated at p_{av}. In terms of the pseudopressure function,

$$q_g = C[m(p_R) - m(p_{wf})], \tag{2.70}$$

where

$$C = \frac{0.703kh}{T[\ln(r_e/r_w) - 0.75 + s]}. \tag{2.71}$$

Equations (2.66) through (2.71) apply to stabilized flow when the Dq_g term is small and can be neglected; $Dq_g \ll [\ln(r_e/r_w) - 0.75 + s]$. At high rates, or when Dq_g has a relatively large effect, the Dq_g term dominates the skin and the resulting low-pressure gas equation (eq. [2.44]) becomes

$$q_g = \left[\frac{0.703kh(p_R^2 - p_{wf}^2)}{T\mu_g ZD}\right]^{0.5} \tag{2.72}$$

or

$$q_g = C(p_R^2 - p_{wf}^2)^{0.5}, \tag{2.73}$$

where

$$C = \left[\frac{0.703kh}{T\mu_g ZD}\right]^{0.5}. \tag{2.74}$$

Similar expressions for C can also be written for pressure and pseudopressure when Dq_g dominates the flow equation. Equations (2.66) through (2.74) apply for the

two limiting conditions of inflow equations; pure Darcy flow ($D = 0$, $n = 1$) and completely turbulent flow ($D = \infty$, $n = 0.5$).

A generalized expression for the backpressure equation that is valid at the two limiting conditions and approximate for the range $0.5 < n < 1.0$ is, for low-pressure gas,

$$q_g = C(p_R^2 - p_{wf}^2)^n, \tag{1.33}$$

where

$$C = \frac{(0.703kh)^n}{(T\mu_g Z)^n D^{1-n}[\ln(r_e/r_w) - 0.75 + s]^{2n-1}}. \tag{2.75}$$

For high-pressure gas wells,

$$q_g = C(p_R - p_{wf})^n, \tag{2.76}$$

where

$$C = \frac{(1.407p_{av}kh)^n}{(T\mu_g Z)^n D^{1-n}[\ln(r_e/r_w) - 0.75 + s]^{2n-1}}. \tag{2.77}$$

Using the pseudopressure function,

$$q_g = C[m(p_R) - m(p_{wf})]^n, \tag{2.78}$$

where

$$C = \frac{(0.703kh)^n}{T^n D^{1-n}[\ln(r_e/r_w) - 0.75 + s]^{2n-1}}. \tag{2.79}$$

Tek, Grove, and Poettman (1957) published alternative expressions for the backpressure constant C if $n < 1$, based on theoretical arguments put forth by Houpeurt (1953). Their work is not widely used by the industry because of a somewhat complicated procedure for determining C. We have found the relations presented here accurate enough for practical applications. Example 2.9 shows the use of equations (1.33) and (2.75) for a gas well in the Hugoton field in Texas.

EXAMPLE 2.9 STABILIZED MULTIRATE TEST ANALYSIS OF THE FREE NO. 4 WELL, HUGOTON FIELD, TEXAS

The Free No. 4 is a low-pressure gas well in the Texas Hugoton field. Cullender [Gas Well No. 1] (1955) and Tek et al. (1957) analyzed test data on the Free No. 4 obtained from 1944 to 1946. Table E2.9a gives relevant reservoir and well data. Using the approximate relation for backpressure constant C in equation (2.75), compare the calculated value with the field constant determined from a 24-hour test (table E2.9b).

EXAMPLE 2.9 continued

Table E2.9a Reservoir and Well Data for the Free No. 4 Well

Net pay thickness h[a]	120 ft
Permeability k[b]	30 md
Reservoir temperature T	90°F
Initial gas viscosity μ_g	0.012 cp
Initial Z-factor Z	0.925
Initial total compressibility c_{ti}	0.0016 1/psi
Gas gravity γ_g	0.712
Wellbore radius r_w	0.292 ft
Skin factor s[b]	−3.2
Backpressure exponent n[b]	0.867
Porosity, ϕ	0.07

[a] The zone was completed open hole with an acid treatment.
[b] Based on evaluation of all the Cullender data.

Table E2.9b 24-hour Test Data for the Free No. 4 Well

Test Reference	p_R (psia)	p_{wf} (psia)	q_g (MMscf/D)	Test C
Cullender				
10-03-44	435.2	302.8	9.900	467.1
10-24-44	436.8	390.0	4.440	467.9
12-11-45	394.7	375.8	1.947	478.5
Tek et al.*	424.0	357.9	5.165	423.2

* Last of four 24-hour rates in a flow after flow sequence.

SOLUTION

Constant C is given by equation (2.75) as

$$C = \frac{[0.703kh/T\mu Z]^n}{D^{1-n}[\ln(r_e/r_w) - 0.75 + s]^{2n-1}}.$$

In section 2.7 it is shown that the transient drainage radius is calculated from equation (2.135) as

$$r_e = 0.024[kt/\phi\mu_i c_{ti}]^{0.5}.$$

For 24-hour isochronal flow periods the drainage radius is

$$r_e = 0.024[(30)(24)/(0.07)(0.012)(0.0016)]^{0.5}$$

$$= 555 \text{ ft}.$$

EXAMPLE 2.9 continued

This yields

$$\ln(r_e/r_w) - 3.2 = \ln(550/0.292) - 3.2$$

$$= 4.3$$

From equation (2.63)

$$D = 2.222 \times 10^{-18} \frac{\gamma_g k h \beta}{\mu_g r_w h_p^2}$$

$$= 2.222 \times 10^{-18} \frac{(0.712)(30)(120)(2.73 \times 10^{10})(30^{-1.1045})}{(0.012)(0.292)(120^2)}$$

$$= 7.19 \times 10^{-8}.$$

Substituting the values of r_e and D in equation (2.75) gives

$$C = \frac{[(0.703)(30)(120)/(550)(0.012)(0.925)]^{0.867}}{(7.19 \times 10^{-8})^{0.133}(4.3)^{0.734}}$$

$$= 568$$

The 24-hour rate–pressure data given by Cullender and by Tek et al. give C values that range from 423 to 479. The calculated C is higher, although it is a good approximation. A permeability of 30 md has been used here, even though Tek et al. report $k = 46.9$ md from a buildup test. The 30 md value was determined from analysis of all the transient data given by Cullender (see example 2.21). Since the Tek et al. analysis uses calculated bottomhole pressures and the buildup follows a four-point flow-after-flow sequence (24 hours each), the accuracy of their analysis can be argued. The calculated $C = 568$ represents the backpressure equation at the end of the 24-hour flow period. Example 2.21 shows that the C value in this well will continue to decrease until pseudosteady state is reached (after 21 days) and C stabilizes.

2.5 RATE–PRESSURE RELATION FOR SATURATED OIL WELLS.

Thus far we have considered the flow of undersaturated oil and gas, both of which are considered homogeneous (single-phase) systems. Most oil wells, however, produce both gas and oil from the reservoir. The most typical two-phase gas/oil system is the solution gas drive reservoir. Gas that is initially dissolved in the oil at reservoir conditions evolves continuously as pressure drops below the bubble point. The free gas pushes the oil toward producing wells as it seeks to occupy more of the pore volume for expansion. After a sufficient gas saturation has developed in the formation the free